CONFIDENTIAL

OFFICE OF SCIENTIFIC RESEARCH & DEVELOPMENT
NATIONAL DEFENSE RESEARCH COMMITTEE
DIVISION SIX - SECTION 6.1

FORCE AND CAVITATION TESTS WESTINGHOUSE HYDROBOMB

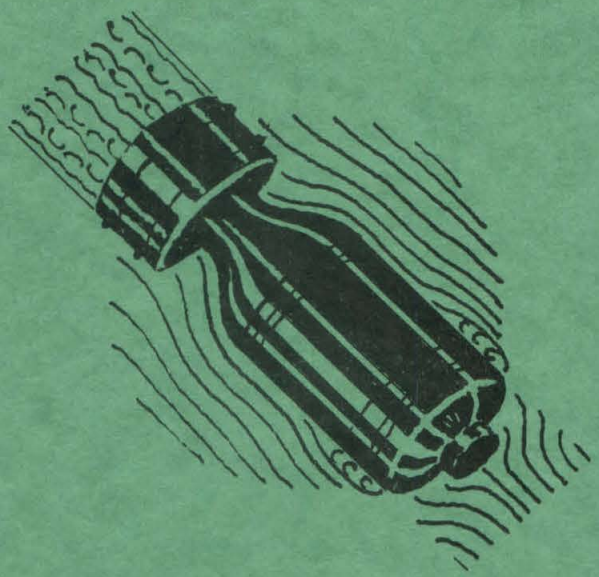

THE HIGH SPEED WATER TUNNEL
CALIFORNIA INSTITUTE OF TECHNOLOGY.
PASADENA, CALIFORNIA

SECTION Nº 6.1 - Sr 207-2234
LABORATORY Nº ND-40

CONFIDENTIAL

COPY Nº 116

OFFICE OF SCIENTIFIC RESEARCH AND DEVELOPMENT
NATIONAL DEFENSE RESEARCH COMMITTEE
DIVISION SIX – SECTION 6.1

FORCE AND CAVITATION TESTS OF THE WESTINGHOUSE HYDROBOMB

ROBERT T. KNAPP

OFFICIAL INVESTIGATOR

THE HIGH SPEED WATER TUNNEL
AT THE
CALIFORNIA INSTITUTE OF TECHNOLOGY
HYDRODYNAMICS LABORATORY
PASADENA, CALIFORNIA

Section No. 6.1-sr207-2234

Laboratory No. ND-40

Report Prepared by
Robert M. Peabody
Hydraulic Engineer

June 27, 1945

TABLE OF CONTENTS

FORCE AND CAVITATION TESTS OF THE WESTINGHOUSE HYDROBOMB

INTRODUCTION

This report covers Water Tunnel tests of a 2" diameter scale model of the Westinghouse Hydrobomb. The results apply only to underwater performance under steady state conditions. No tests were made to determine damping characteristics. The tests reported herein were authorized by a letter dated January 29, 1944, from Dr. E. H. Colpitts, Chief of Section 6.1, National Defense Research Committee.

RESULTS AND CONCLUSIONS

The model test results indicate that, with suitably adjusted rudder settings and control, the underwater running performance of the Westinghouse Hydrobomb should be satisfactory. The drag coefficient, extrapolated to a prototype speed of 40 knots, has the same value as that given by model tests of the Mk 13 Torpedo, extrapolated to a prototype speed of 40.5 knots.

The hydrobomb is statically unstable near zero pitch or yaw, and the instability is greater in yaw than in pitch.

The effect of the depth rudders on moment is about three times that of the course rudders.

For the same rudder angles, both the course and depth rudders are considerably more effective than the rudders of the Mk 13.(1)

Cavitation tests indicate that for underwater running at 40 knots and 10 feet submergence, the hydrobomb would be free from severe cavitation at yaws up to 6°. Observation of the fully developed cavitation bubble shows that the bubble is not symmetrical at other than zero yaw. It is suggested that a nose with a spherical tip will give an entry bubble that is symmetrical and less sensitive to entry pitch or yaw.

PURPOSE AND SCOPE OF TESTS

This report covers the results of High Speed Water Tunnel tests made in the Hydrodynamics Laboratory at the California Institute of Technology on a model of the Westinghouse Hydrobomb.

(1) "Water Tunnel Tests of the Mk 13-1, Mk 13-2, and Mk 13-2A Torpedoes," Section No. 6.1-sr207-936, by Robert T. Knapp, November 9, 1943

The purposes of the tests were the following:

1. To determine the hydrodynamic forces acting on the hydrobomb under conditions of steady state underwater running as functions of speed, projectile orientation, and rudder setting.

2. To determine the cavitation characteristics of the hydrobomb as affected by speed, depth, and orientation.

Tests were made in the pitching plane at angles of attack from 0° to $\pm 8^\circ$, and with depth rudders neutral, 10° up and 10° down. In the yawing plane, tests were made at yaw angles from 0° to $\pm 12^\circ$, with course rudders neutral and 10° port.

Cavitation tests were made to determine the pressures and speeds at which cavitation commenced on various parts of the hydrobomb, and to indicate the appearance of the hydrobomb under extreme cavitation conditions such as would occur at high speed water entry.

Definitions and symbols are given in the appendix.

DESCRIPTION OF HYDROBOMB AND MODEL

The Westinghouse Hydrobomb is a jet-propelled aerial torpedo with four stabilizing fins, vertical rudders for course control, and horizontal rudders for depth control. The rudder control mechanism for both course and depth control is of the "bang-bang" type, that is, the course rudders act under direction-responsive control from hard port to hard starboard, and the depth rudders, under control responsive to both pitch and depth, act from hard up to hard down.

The hydrobomb nose is a streamlined form closely approximating a semiellipsoid, with a ratio of major to minor axes of 1.9 to 1.0.

The afterbody profile is tangent to the central cylindrical section and tapers with gradually increasing curvature in a length of 48.5 inches from the body diameter of 22.42 inches to the small end diameter of 6.23 inches. The two course fins are unequal, the lower fin extending 1 inch farther from the projectile axis than the upper. The two depth fins have equal dimensions, but the total span of the depth fins is 30 inches or about 6-1/2 inches greater than the span of the course fins. The area of the depth fins is about 40 per cent more than the course-control fins.

The fins themselves are streamlined, rounded on the leading and outer edges and tapering from a thickness of 1/2 inch at the leading and outer edges to a maximum thickness of 2 inches where they are attached to the afterbody.

Figure 1 is a side view of the model showing the course fins and rudders; Figure 2 is a top view showing the depth fins and

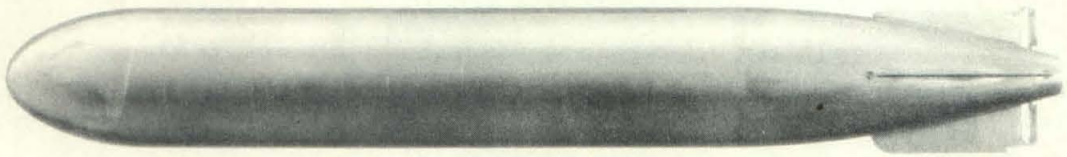

FIG. 1 – SIDE VIEW – WESTINGHOUSE HYDROBOMB

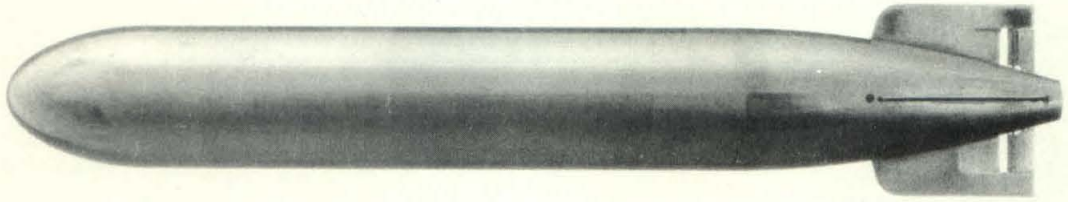

FIG. 2 – TOP VIEW – WESTINGHOUSE HYDROBOMB

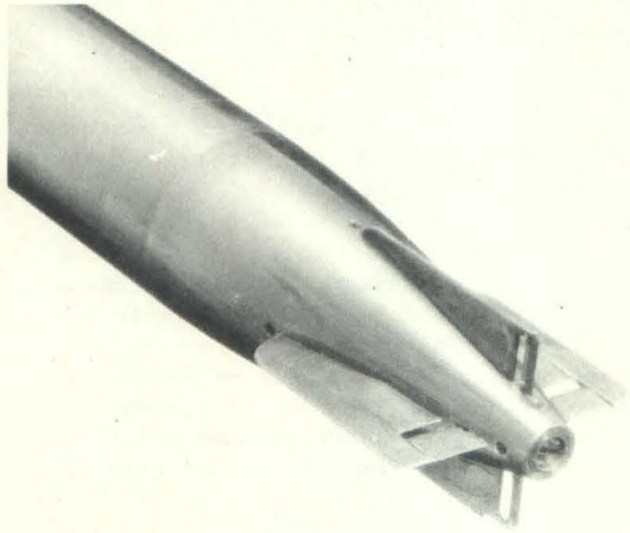

FIG. 3
AFTERBODY AND FINS
WESTINGHOUSE HYDROBOMB

rudders; and Figure 3 shows the afterbody, fins, and rudders in more detail.

The principal dimensions of the hydrobomb are shown in Figure 4.

The model tested was 2 inches in diameter, constructed to a linear scale ratio to the prototype of 1 to 11.21.

The principal dimensional characteristics are the following:

	Model	Prototype
Overall Length	14.284 in.	160.125 in.
Maximum Diameter	2.00 in.	22.42 in.
Nose to Center of Buoyancy		73 in.
Nose to Center of Gravity		
Motor Loaded		68.2 in.
Motor Empty		74.5 in.
Weight, Motor Loaded		2360 lb.
Negative Buoyancy		590 lb.

TEST PROCEDURE - FORCE TESTS

The hydrodynamic characteristics determined by the model tests are expressed in terms of drag, lift (or cross force) and moment coefficients calculated from the observed forces and moments.

For the force and moment measurements, the model is mounted on a shielded spindle in the working section of the water tunnel. The spindle, to which the model is rigidly attached, is extended outside the tunnel working section and connected to balances which measure the forces and moments. The shield which surrounds the mounting spindle in the working section is streamlined and extends to within a few thousandths of an inch of the model, thus protecting the spindle from the tunnel flow. To compensate for interference between the shield and the model, each series of tests is repeated with an image shield extending from the top of the working section to the same clearance from the model as the spindle shield. The image shield is a mirror duplicate of the spindle shield.

A tare or shield interference correction is then applied in accordance with standard wind tunnel practice as follows:

$$F = F_o - (F_w - F_o)$$

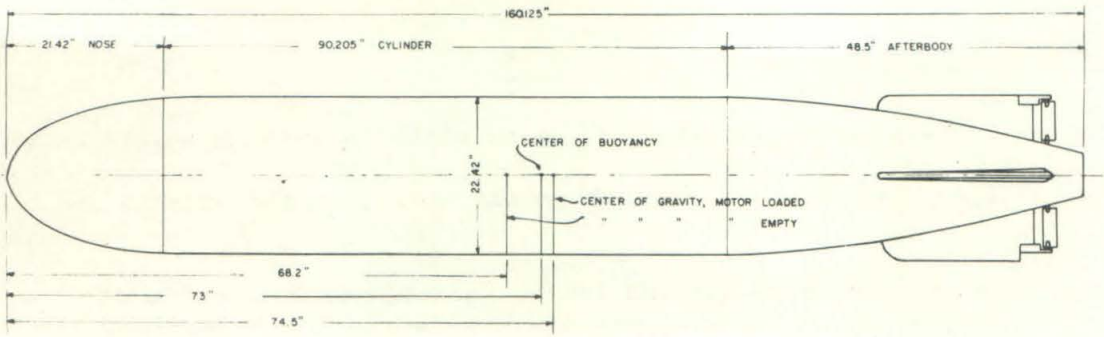

REF: WESTINGHOUSE ELEC. & MFG. CO.
E D SK 173598

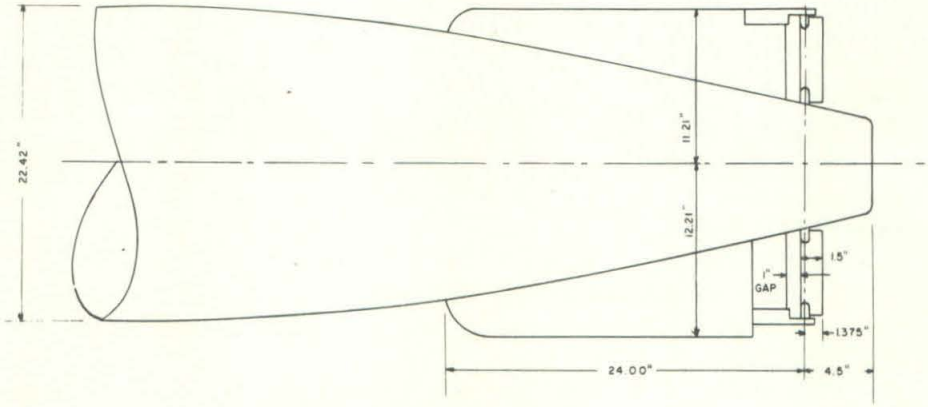

SIDE VIEW SHOWING COURSE RUDDERS

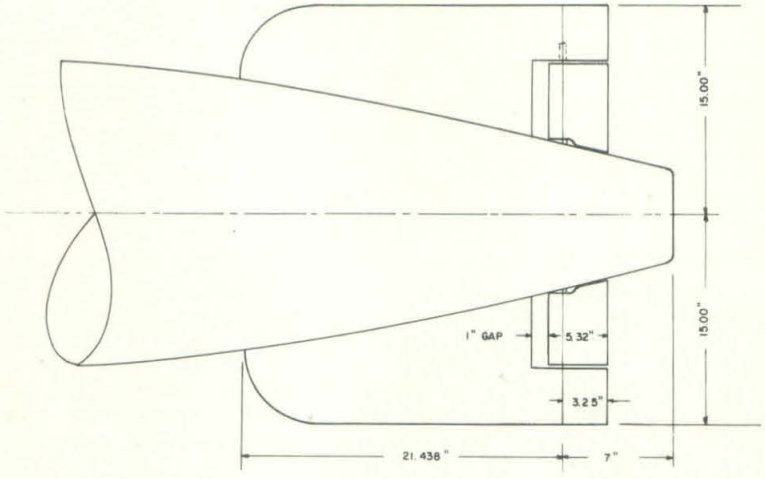

TOP VIEW SHOWING DEPTH RUDDERS

FIG. 4 — OUTLINE DIMENSIONS
WESTINGHOUSE HYDROBOMB

where

F = the corrected force or moment

F_o = the measured force or moment with the spindle shield only

F_w = the measured force or moment with both the spindle and image shields

A correction is applied to the measured drag to allow for the tunnel pressure gradient, which was measured in the working section of the tunnel in the absence of the model. The pressure gradient dp/dx at each station was multiplied by the cross-sectional area of the model at that station and the product plotted against distance along the model. The correction is then the area under this curve which can be expressed as

$$\int_o^L S \frac{dp}{dx} dx = \int_o^L S \, dp$$

where

S = cross-sectional area of model at a station where, in the absence of the model, the pressure would be p.

The resulting correction to be subtracted from the measured drag coefficient was found to be 0.012, or about 9 per cent of the measured value.

Each series of yawing and pitching tests, both with and without the image shield, was repeated with the afterbody of the model rotated 180 degrees from its position in the first series. Averaging the values of the tests in these two positions tends to compensate for the effect of any accidental asymmetry in the model.

DRAG MEASUREMENTS

The results of the drag measurements are shown in Figure 5, where drag coefficient is plotted as a function of Reynolds number. The test runs were made at water velocities of from 10 to 60 ft/sec in steps of about 5 ft/sec. All test runs were made with the torpedo in normal running position with the course fins vertical and at zero pitch and yaw. Each series of runs from 10 to 60 ft/sec was repeated with the afterbody rotated 180 degrees, and each of these two series repeated with the image shield in place. The curve of Figure 5 shows all of the test points after correcting for shield interference and tunnel pressure gradient (horizontal buoyancy). The curve is a straight line on log-log paper. As an interesting comparison, the von Karman curve for turbulent skin friction only, for a flat plate of the same surface area and length as the hydrobomb, has also been plotted in Figure 5.

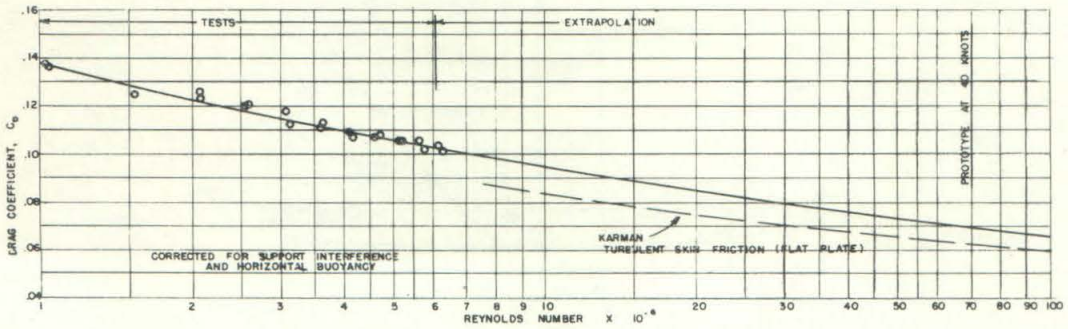

FIG. 5 – DRAG COEFFICIENT VS. REYNOLDS NUMBER
WESTINGHOUSE HYDROBOMB

As may be seen from the figure, the range of the tests covered Reynolds numbers between about 1.1×10^6 and 6.3×10^6, whereas the Reynolds number for the prototype at 40 knots is 70×10^6. Extrapolation over such a wide range is not completely reliable. The results so obtained are useful for preliminary estimating purposes, in the absence of confirming data from actual runs on the full size torpedo.

LIFT, CROSS FORCE, AND MOMENT MEASUREMENTS

Pitch – Figure 6 shows the lift and drag coefficients as functions of the angle of attack, or pitch angle, for depth rudders at 0°, 10° up and 10° down. Figure 7 shows the moment coefficient curves for the hydrobomb with the motor loaded and empty.

Yaw – Figure 8 shows cross force, and Figure 9 shows moment coefficients of the hydrobomb as functions of yaw. Figure 9 shows the moment coefficient curves, both for the motor loaded and motor empty.

The slopes of the moment curves at zero pitch and yaw are positive, indicating static instability at small deviations from zero pitch and yaw. In pitch the positive slope is considerably less than in yaw, indicating that, at small pitch angles, the hydrobomb is less unstable than at small yaw angles.

The effect of 10° movement of the depth rudders on the moment at zero pitch is approximately three times the effect of the smaller course rudders on the moment at zero yaw. At larger angles the comparative effect of the depth rudders is greater.

The drag, force, and moment characteristics for steady state conditions shown on Figures 5 to 9 are not sufficient to determine the dynamic stability of the free-running hydrobomb without additional information as to the damping forces and moments, which is not covered by this report.

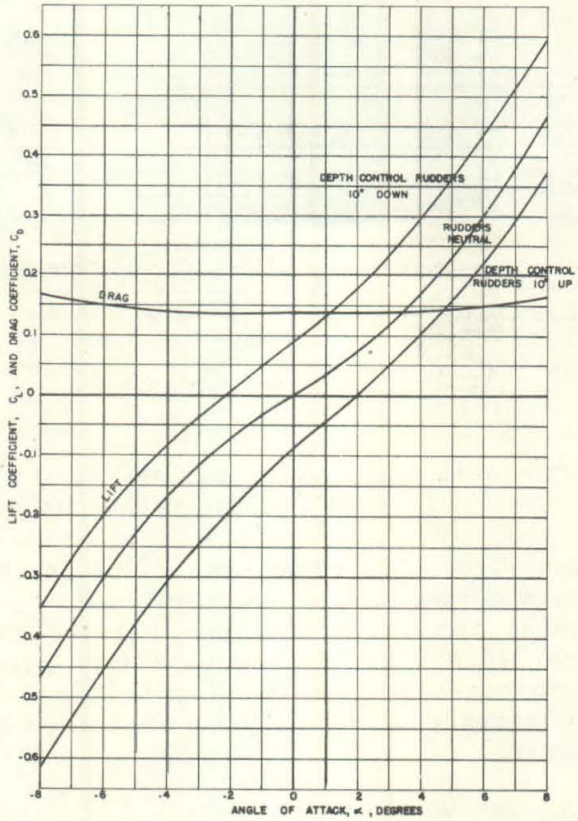

FIG. 6 — DRAG AND LIFT COEFFICIENTS
VS. ANGLE OF ATTACK
WESTINGHOUSE HYDROBOMB

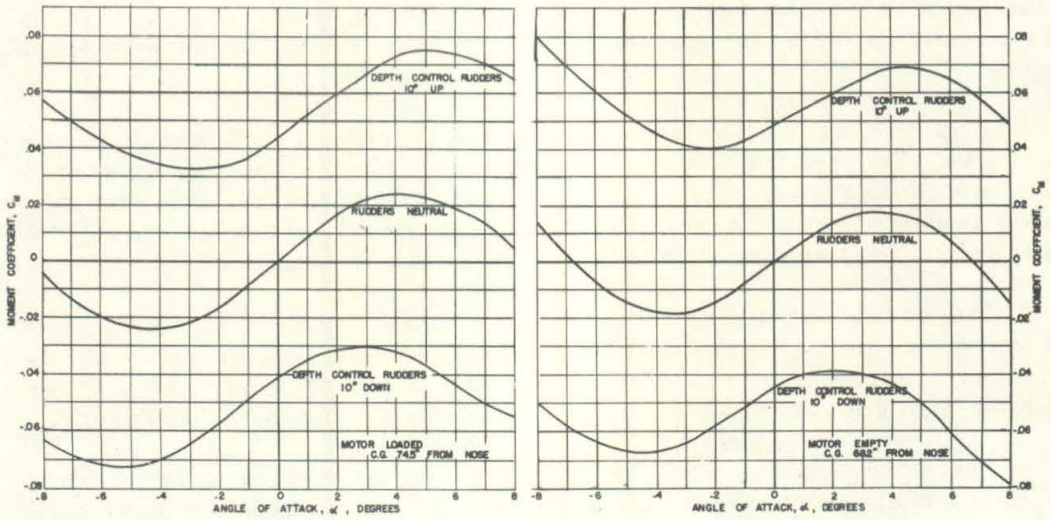

FIG. 7 — MOMENT COEFFICIENT VS. ANGLE OF ATTACK
WESTINGHOUSE HYDROBOMB

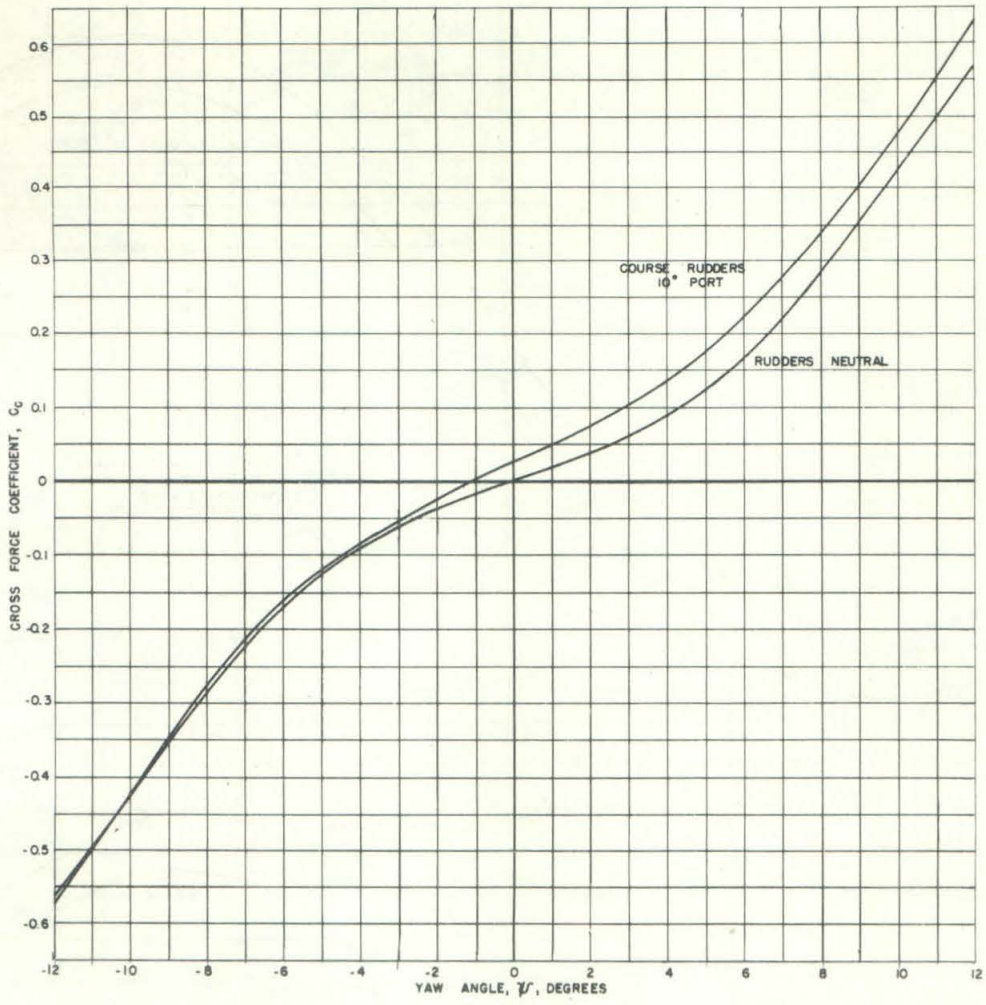

FIG. 8 – CROSS FORCE COEFFICIENT VS. YAW
WESTINGHOUSE HYDROBOMB

Referring to the details of the fins and rudders shown on Figure 4, it will be noted that there is a gap of 1 inch between the forward edges of the rudders and the aft edges of the fins. It was thought that the existence of this gap might have an adverse effect on the rudder action, so fillers of the same thickness as the rudders were attached to and faired into the fins, extending aft to just clear the rudders, and the moment tests were repeated. The effect on performance was found to be either negligible or within the range of accuracy of the tests.

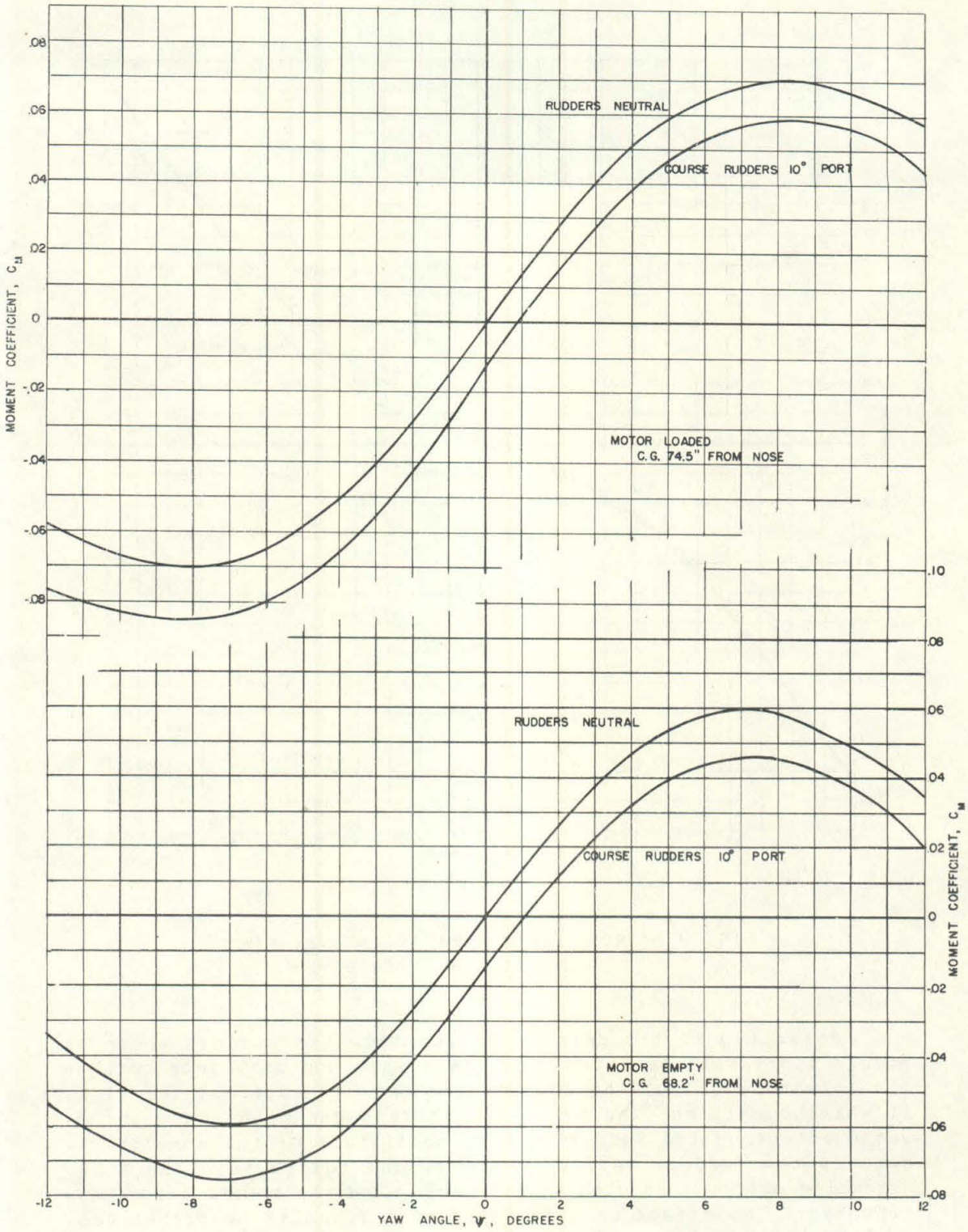

FIG. 9 — MOMENT COEFFICIENT VS. YAW
WESTINGHOUSE HYDROBOMB

CAVITATION

Cavitation tests were conducted to determine the pressure and velocity at which cavitation appeared on the nose and fins of the hydrobomb, and to observe the more fully developed cavitation bubble at conditions of high velocity and low pressure such as occur in the water entry phase.

The cavitation results are expressed in terms of the cavitation parameter, K, as defined in the appendix.

In the cavitation tests, the model torpedo in the water tunnel was subjected to a water velocity of 57 to 60 ft/sec. From an initial pressure (p_L) high enough to prevent any observable cavitation, the pressure was gradually reduced until cavitation developed.

Steady incipient cavitation was observed to occur at the K values shown in the following tabulation:

	Values of K for Incipient Cavitation		
	0° Yaw	3° Yaw	6° Yaw
Nose	0.31	0.37	0.41
Rudders or Rudder Supports	0.41	0.53	0.57
Leading edge of Fin	0.80	0.86	1.14

The submergence necessary to avoid any cavitation at these various points at a speed of 40 knots is given below:

	Submergence, in feet, necessary to avoid cavitation at 40 knots		
	0° Yaw	3° Yaw	6° Yaw
Nose	0	0	0
Rudders or Rudder Supports	0	5	8
Leading edge of Fin	24	28	44

Five feet submergence corresponds to a K value of 0.54 at 40 knots. Observation of the hydrobomb in the water tunnel at this K value indicates that the fin cavitation, while well developed, is not severe enough to have much effect on the rudders, although it may possibly increase the drag somewhat. The top photograph of Figure 12 shows the fin cavitation at 6 degrees yaw, at a K value of 0.36, corresponding to zero submergence at 40 knots.

K = 0.32

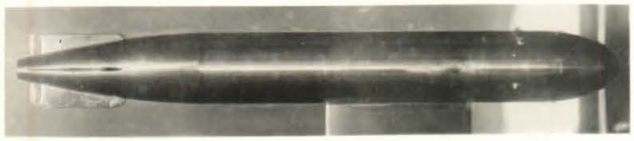

K = 0.29

K = 0.24

K = 0.19

FIG. 10 — DEVELOPMENT OF CAVITATION AT ZERO YAW

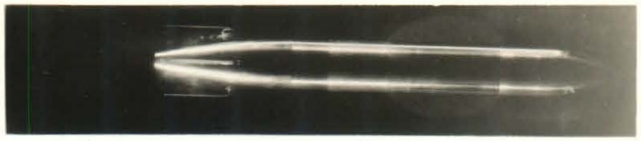

K = 0.34

K = 0.29

K = 0.25

K = 0.18

FIG. 11 — DEVELOPMENT OF CAVITATION AT 3° YAW

WESTINGHOUSE HYDROBOMB

Figures 10, 11, and 12 are photographs showing the development of cavitation from inception to nearly full bubble at 0°, 3°, and 6° yaw.

The photographs in Figure 10 (zero yaw) were taken with the camera in the plane in which the model is yawed. Figures 11 and 12 were made with the camera perpendicular to the yaw plane. The K values are noted on each picture.

In each of the figures, the lower photograph shows the appearance of the cavitation bubble as it nearly encloses the entire projectile. The orientation of the line of contact between the bubble and the nose of the projectile is especially to be noted, particularly the difference observable between zero yaw and 3° and 6° yaw.

In all the photographs, the direction of flow is parallel to the top and bottom edges of the pictures. At zero yaw, the line of contact of bubble and nose is perpendicular to the direction of flow. At 3° yaw, the contact line is at an angle of about 9° to a line perpendicular to the flow, and at 6° yaw angle is about 18°.

K = 0.36

K = 0.26

K = 0.21

K = 0.17

FIG. 12 — DEVELOPMENT OF CAVITATION AT 6° YAW

WESTINGHOUSE HYDROBOMB

Yaw = 0° K = 0.22

Yaw = 3° K = 0.22

Yaw = 6° K = 0.23

FIG. 13 — CAVITATION BUBBLE ON A PROJECTILE WITH HEMISPHERICAL NOSE

Figure 13 shows a cavitating projectile with a hemispherical nose at yaws of 0°, 3°, and 6°. It is to be noted that the line of contact between bubble and nose is perpendicular to the flow regardless of yaw.

There is reason to believe that a nose shape which will, for small yaws, hold the contact line between bubble and nose closely perpendicular to the direction of flow, will make a water entry projectile less sensitive to the effect of entry pitch or yaw on the underwater trajectory. For a further discussion of this subject, reference is made to a report by Dr. Robert T. Knapp entitled "Entrance and Cavitation Bubbles", Section No. 6.1-sr207-1900, filed in the Office of Scientific Research and Development.

As brought out on page 39 of that report, it appears possible for a spherogive nose to be designed which will give nearly as good underwater performance as a finer ellipsoidal nose, and probably better performance at entry. This possibility is illustrated by Figure 14 which shows a comparison of the nose shape of the Westinghouse Hydrobomb with a 2.3 caliber, 72° spherogive nose that has been investigated at zero yaw in the High Speed Water Tunnel.

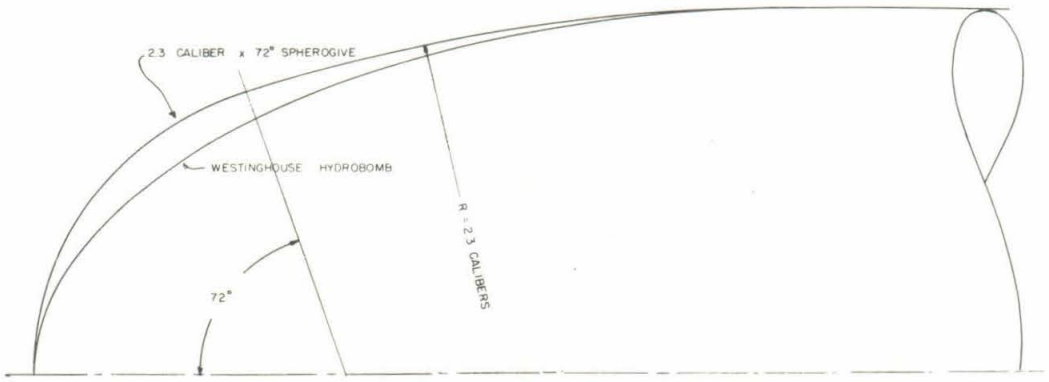

	WESTINGHOUSE HYDROBOMB	2.3 x 72° SPHEROGIVE
"K" FOR INCIPIENT CAVITATION ON NOSE	0.31	0.35
MAX. SPEED, KNOTS, WITHOUT NOSE CAVITATION AT 10 FT SUBMERGENCE	55.8	54.3
NOSE VOLUME COEFFICIENT	0.67	0.72

FIG. 14 – COMPARISON OF NOSE PROFILES

This nose has a spherical tip of 0.40 caliber radius, tangent to the 2.3 caliber ogive radius at 72° from the longitudinal axis. The cavitation parameter, K, for incipient cavitation at zero yaw is 0.35 and the cavitation definitely occurs on the spherical tip. Tests in the Water Tunnel on various spherogive noses indicate that cavitation occurs on the sphere when the point of tangency of sphere with ogive is more than 68° to 70° from the axis. The line of contact of the cavitation bubble with the 2.3 x 72° nose should remain on the spherical tip for yaws up to about 2°. Therefore, at small yaws the bubble would remain symmetrical and there would be no side forces on the nose during the bubble phase of entry.

FLOW PATTERNS

Figures 15 to 18, inclusive, are drawings of flow patterns made from observation of the fluid motion about the afterbody and fins in the Polarized Light Flume. The fluid in the flume has asymmetrical physical and optical properties which permit observation of the flow lines when viewed through polarizing plates. The pictures are for flow velocities below the range of the water tunnel tests and the patterns can be considered only qualitative.

Figures 15 and 16 indicate that separation of the flow from the afterbody occurs only aft of the rudders. As may be seen in Figure 16, the fins at zero pitch cause very little disturbance of flow. Figures 17 and 18 show flow separation and eddies on the upper side of the horizontal fin. It is to be noted also, in Figures 17 and 18, that at 10° pitch there is a distinct upward flow through the gap between the fin and rudder. However, as mentioned earlier in this report, force measurements did not show any appreciable difference when this gap was closed.

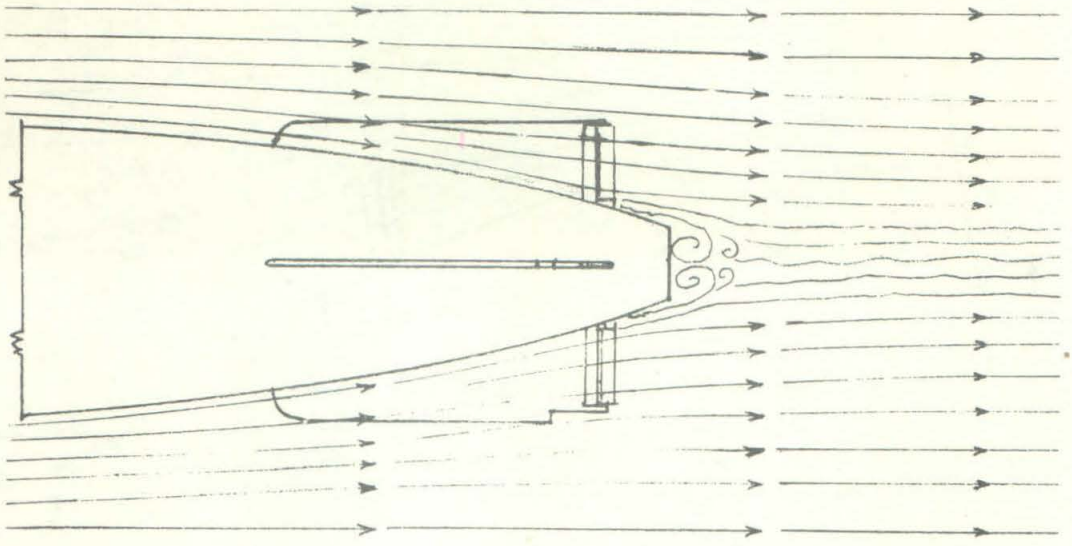

FIG. 15 – FLOW PATTERN AT ZERO PITCH, NEUTRAL RUDDER

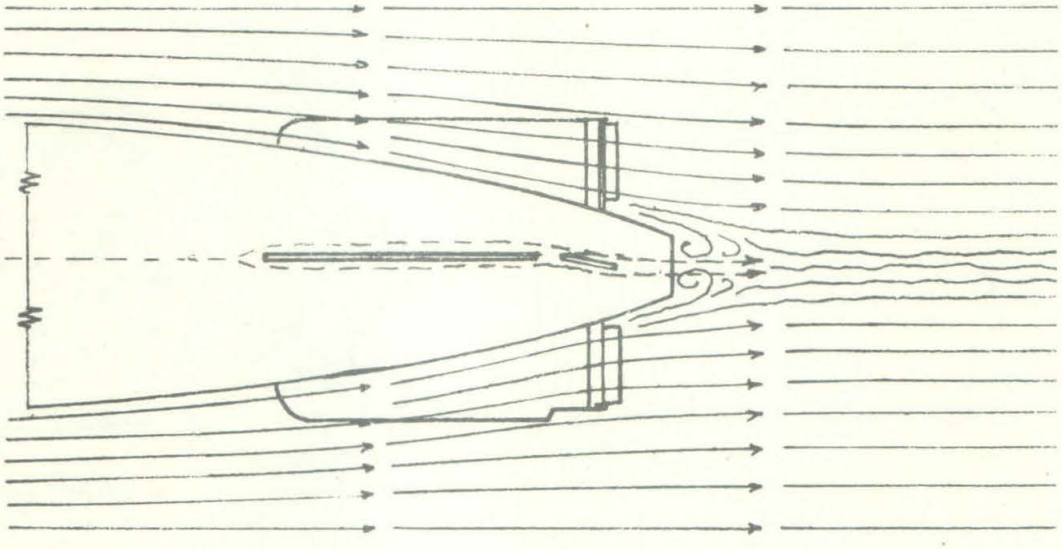

FIG. 16 – FLOW PATTERN AT ZERO PITCH, 10^{o} DOWN RUDDER

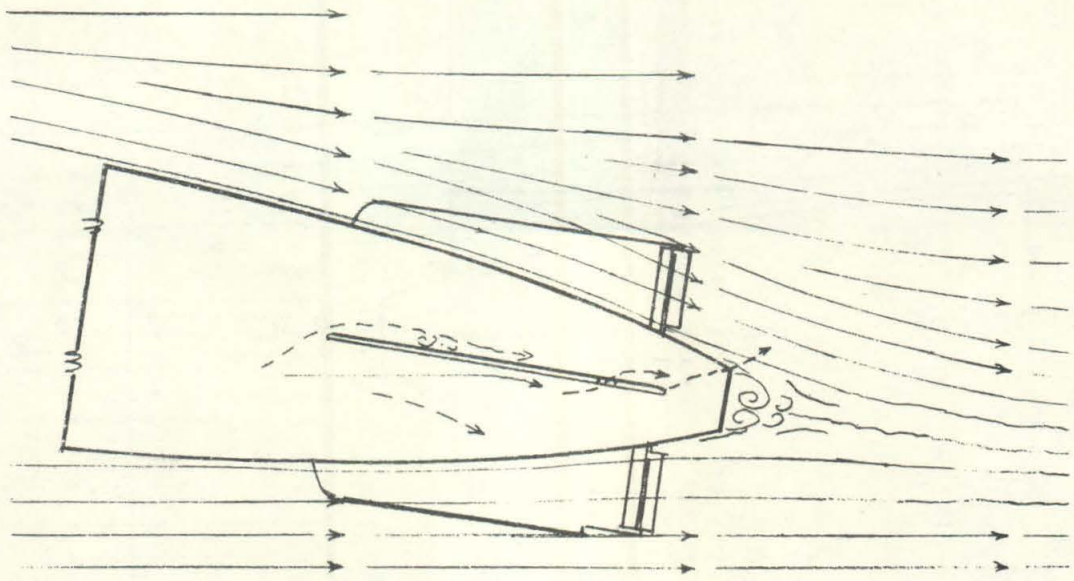

FIG. 17 – FLOW PATTERN AT 10^{0} PITCH, NEUTRAL RUDDER

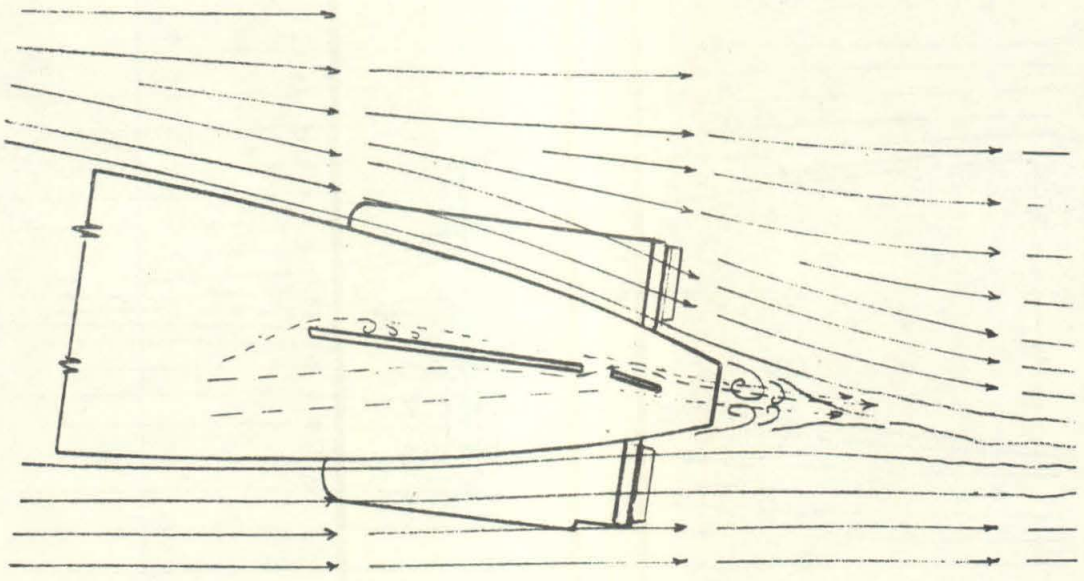

FIG. 18 – FLOW PATTERN AT 10^{0} PITCH, 10^{0} DOWN RUDDER

APPENDIX

DEFINITIONS

YAW ANGLE, ψ

The angle, in a horizontal plane, which the axis of the projectile makes with the direction of motion. Looking down on the projectile, yaw angles in a clockwise direction are positive (+) and in a counterclockwise direction, negative (−).

PITCH ANGLE, α

The angle, in a vertical plane, which the axis of the projectile makes with the direction of motion. Pitch angles are positive (+) when the nose is up and negative (−) when the nose is down.

LIFT, L

The force, in pounds, exerted on the projectile normal to the direction of motion and in a vertical plane. The lift is positive (+) when acting upward and negative (−) when acting downward.

CROSS FORCE, C

The force, in pounds, exerted on the projectile normal to the direction of motion and in a horizontal plane. The cross force is positive when acting in the same direction as the displacement of the projectile nose for a positive yaw angle, i.e., to an observer facing in the direction of travel, a positive cross force acts to the right.

DRAG, D

The force, in pounds, exerted on the projectile parallel with the direction of motion. The drag is positive when acting in a direction opposite to the direction of motion.

MOMENT, M

The torque, in foot pounds, tending to rotate the projectile about a transverse axis. Yawing moments tending to rotate the projectile in a clockwise direction (when looking down on the projectile) are positive (+), and those tending to cause counterclockwise rotation are negative (−). Pitching moments tending to rotate the projectile in a clockwise direction (when looking at the projectile from the port side) are positive (+), and those tending to cause counterclockwise rotation are negative (−).

In accordance with this sign convention a moment has a destabilizing effect when it has the same sign as the yaw or pitch angle.

In all model tests the moment is measured about the point of support. Moments about the center of gravity of the projectile have the symbol, M_{cg}.

NORMAL COMPONENT, N

The sum of the components of the drag and cross force acting normal to the axis of the projectile. The value of the normal component is given by the following:

$$N = D \sin \psi + C \cos \psi \qquad (1)$$

in which

N = Normal component in lbs.

D = Drag in lbs

C = Cross force in lbs

ψ = Yaw angle in degrees

CENTER OF PRESSURE, CP

The point in the axis of the projectile at which the resultant of all forces acting on the projectile is applied.

CENTER-OF-PRESSURE ECCENTRICITY, e

The distance between the center of pressure (CP) and the center of gravity (CG) expressed as a decimal fraction of the length (l) of the projectile. The center-of-pressure eccentricity is derived as follows:

$$e = (l_{cp} - l_{cg}) \frac{1}{l} = \frac{1}{l} \frac{Mcg}{N} \qquad (2)$$

in which

e = Center-of-pressure eccentricity

l = Length of projectile in feet

l_{cg} = Distance from nose of projectile to CG in feet

l_{cp} = Distance from nose of projectile to CP in feet

COEFFICIENTS

The three force and moment coefficients used are derived as follows:

Drag coefficient, $$C_D = \frac{D}{\rho \frac{V^2}{2} A_D} \quad (3)$$

Cross force coefficient, $$C_C = \frac{C}{\rho \frac{V^2}{2} A_D} \quad (4)$$

Lift coefficient, $$C_L = \frac{L}{\rho \frac{V^2}{2} A_D} \quad (4a)$$

Moment coefficient, $$C_M = \frac{M}{\rho \frac{V^2}{2} A_D l} \quad (5)$$

in which

D = Measured drag force in lbs.

C = Measured cross force in lbs

L = Measured lift force in lbs

ρ = Density of the fluid in slugs/cu ft = w/g

w = Specific weight of the fluid in lbs/cu ft

g = Acceleration of gravity in ft/sec^2

A_D = Area in sq ft at the maximum cross section of the projectile taken normal to the geometric axis of the projectile

V = Mean relative velocity between the water and the projectile in ft/sec

M = Moment, in foot-pounds, measured about any particular point on the geometric axis of the projectile

l = Overall length of the projectile in feet

RUDDER EFFECT

The total increase or decrease in moment coefficient, at a given yaw or pitch angle, resulting from a given rudder setting. This increase or decrease in moment coefficient is measured from the moment coefficient curve for neutral rudder setting.

REYNOLDS NUMBER

In comparing hydraulic systems involving only friction and inertia forces, a factor called Reynolds number is of great utility. This is defined as follows:

$$R = \frac{lV}{\nu} = \frac{lV\rho}{\mu} \qquad (6)$$

in which

R = Reynolds number

l = Overall length of projectile, feet

V = Velocity of projectile, feet per sec

ν = Kinematic viscosity of the fluid, sq ft per sec = μ/ρ

ρ = Mass density of the fluid in slugs per cu ft

μ = Absolute viscosity in pound-seconds per sq ft

Two geometrically similar systems are also dynamically similar when they have the same value of Reynolds number. For the same fluid in both cases, a model with small linear dimensions must be used with correspondingly large velocities. It is also possible to compare two cases with widely differing fluids provided l and V are properly chosen to give the same value of R.

CAVITATION PARAMETER

In the analysis of cavitation phenomena, the cavitation parameter has been found very useful. This is defined as follows:

$$K = \frac{P_L - P_B}{\rho \frac{V^2}{2}} \qquad (7)$$

in which

K = Cavitation parameter

P_L = Absolute pressure in the undisturbed liquid, lbs/sq ft

P_B = Vapor pressure corresponding to the water temperature, lbs/sq ft

V = Velocity of the projectile, ft/sec

ρ = mass density of the fluid in slugs per cu ft = w/g

w = weight of the fluid in lbs per cu ft

g = acceleration of gravity

Note that any homogeneous set of units can be used in the computation of this parameter. Thus, it is often convenient to express this parameter in terms of the head, i.e.,

$$K = \frac{h_L - h_B}{\frac{V^2}{2g}} \qquad (8)$$

where

h_L = Submergence plus the barometric head, ft of water

h_B = Pressure in the bubble, ft of water

It will be seen that the numerator of both expressions is simply the net pressure acting to collapse the cavity or bubble. The denominator is the velocity pressure. Since the entire variation in pressure around the moving body is a result of the velocity, it may be considered that the velocity head is a measure of the pressure available to open up a cavitation void. From this point of view, the cavitation parameter is simply the ratio of the pressure available to collapse the bubble to the pressure available to open it. If the K for incipient cavitation is considered, it can be interpreted to mean the maximum reduction in pressure on the surface of the body measured in terms of the velocity head. Thus, if a body starts to cavitate at the cavitation parameter of one, it means that the lowest pressure at any point on the body is one velocity head below that of the undisturbed fluid.

The shape and size of the cavitation bubbles for a specific projectile are functions of the cavitation parameter. If p_B is taken to represent the gas pressure within the bubble instead of the vapor pressure of the water, as in normal investigations, the value of K obtained by the above formula will be applicable to an air bubble. In other words, the behavior of the bubble will be the same whether the bubble is due to cavitation, the injection of exhaust gas, or the entrainment of air at the time of launching.

The cavitation parameter for incipient cavitation has the symbol K_i.

The following chart gives values of the cavitation parameter as a function of velocity and submergence in sea water.

GENERAL DISCUSSION OF STATIC STABILITY

Water tunnel tests are made under steady flow conditions, consequently the results only indicate the tendency of the steady state hydrodynamic couples and forces to cause the projectile to return to or move away from its equilibrium position after a

disturbance. Dynamic couples and forces including either positive or negative damping are not obtained. If the hydrodynamic moments are restoring the projectile, then it is said to be statically stable, if nonrestoring, statically unstable. In the discussion of static stability the actual motion following a perturbation is not considered at all. In fact, the projectile may oscillate continuously about an equilibrium position without remaining in it. In this case it would be statically stable, but would have zero damping and hence, be dynamically unstable. With negative damping a projectile would oscillate with continually increasing amplitude following an initial perturbation even though it were statically stable. Equilibrium is obtained if the sum of the hydrodynamic, buoyant, and propulsive moments equal zero. In general, propulsive thrusts act through the center of gravity of the projectile so only the first two items are important.

If a projectile is rotating from its equilibrium position so as to increase its yaw angle positively, the moment coefficient must increase negatively (according to the sign convention adopted) in order that it be statically stable. Therefore, for projectiles without controls or with fixed control surfaces, a negative slope of the curve of moment coefficient vs yaw gives static stability and a positive slope gives instability. For a projectile without controls, static stability is necessary for a successful flight unless stability is obtained by spinning as in the case of rifle shells. For a projectile with controls, stabilizing moments can be obtained by adjusting the control surfaces, and the slope of the moment coefficient, as obtained with fixed rudder position, need not give static stability. Where buoyancy either acts at the center of gravity or can be neglected, equilibrium is obtained when the hydrodynamic moment coefficient equals zero. For symmetrical projectiles this occurs at zero yaw angle, i.e., when the projectile axis is parallel to the trajectory. For nonsymmetrical projectiles, such as a torpedo when the rudders are not neutral, the moment is not zero at zero yaw but vanishes at some definite angle of attack. Where buoyancy cannot be neglected equilibrium is obtained when $C_M = -C_{Buoyancy}$, and the axis of the projectile is at some angle with the trajectory.

For symmetrical projectiles the degree of stability, or instability can be obtained from the center-of-pressure curves. If the center of pressure falls behind the center of gravity, a restoring moment exists giving static stability. If the center of pressure falls ahead of the center of gravity, the moment is nonrestoring, and the projectile will be statically unstable. The degree of stability or instability is indicated approximately by the distance between the center of gravity and the center of pressure. In general, for nonsymmetrical projectiles, the cross force or lift is not zero when the moment vanishes so that the center of pressure curve is not symmetrical and the simple rules just stated cannot be used to determine whether or not the projectile will be stable. In such cases careful interpretation of the moment curves is a more satisfactory method of determining stability relationship.

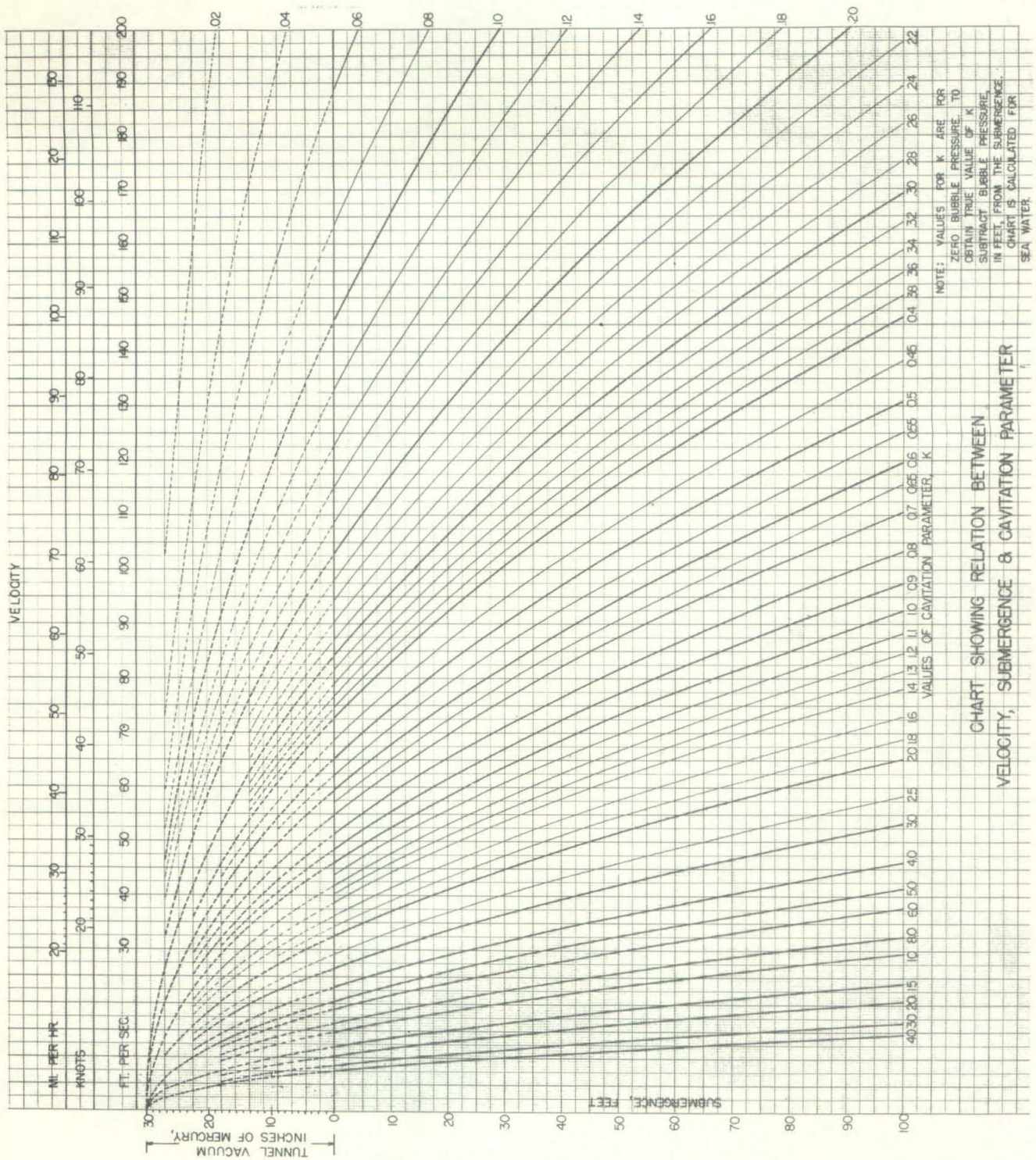

CHART SHOWING RELATION BETWEEN
VELOCITY, SUBMERGENCE & CAVITATION PARAMETER